Supplementary Figure 1. Biosynthesis of DNA Pyrimidines from Glutamine. *De novo* pathway of pyrimidine biosynthesis in mammalian cells. GLS1, glutaminase 1; CPS-II, carbamoyl-phosphate synthetase II; ACTase, aspartate transcarbamoylase; OMP, orotidine monophosphate; UMP, uridine monophosphate; PRPP, 5-phosphoribosyl pyrophosphate.

Supplementary Figure 2. Three Distinct Sources of Aspartate Biosynthesis. (A-D) Aspartate labeling patterns: aspartate biosynthesis through glutamine oxidation in the presence of [U-$^{13}C_5$] glutamine (A), reductive carboxylation in the presence of [1-$^{13}C_1$] glutamine (B), glucose oxidation in the presence of [U-$^{13}C_6$] glucose through PDH (C), or PC (D). PDH, pyruvate dehydrogenase; PC, pyruvate carboxylase.

Supplementary Figure 3. GLS1 Inhibitor BPTES Selectively Suppresses *de novo* Pyrimidine Synthesis in *VHL*$^{-/-}$ cells. (A) Mass Isotopomer Distribution of IMP from [U-$^{13}C_5$] glutamine in RCC Cells. Isogenic *VHL*$^{-/-}$ and *VHL*$^{+/+}$ UMRC2 cells were treated with 2 μM BPTES (for 48 hours) and labeled with [U-$^{13}C_5$] glutamine. The enrichment of the purine precursor inosine monophosphate (IMP) was determined by LC-MS/MS. (B) Ratio of the pyrimidine precursors N-carbamoyl-L-aspartate to carbamoyl phosphate in isogenic *VHL*$^{-/-}$ and *VHL*$^{+/+}$ UMRC2 cells treated with 2 μM BPTES (for 48 hours) or DMSO vehicle control.

Supplementary Figure 4. GLS1 Inhibitors Promote Glucose Oxidation in *VHL*$^{+/+}$ RCC Cells. Isogenic *VHL*$^{-/-}$ and *VHL*$^{+/+}$ UMRC3 cells were labeled with [U-$^{13}C_6$] glucose with or without BPTES at the indicated concentrations (for 48 hours) and the metabolite enrichment was measured by GC-MS. (A-C) Effect of BPTES on the contribution of glucose oxidation, determined by the level of M2 (A) and M3 (B) enriched TCA cycle intermediates, and of citrate enrichment (C) in UMRC3 cells. Student's *t*-test compared BPTES-treated to corresponding control cells. Suc, succinate; Fum, fumarate; α-KG, α-ketoglutarate; Mal, malate; Asp, aspartate; Glu, glutamate.

Supplementary Figure 5. ROS Enhancement Synergizes with GLS1 Inhibitors to Suppress Cell Growth in *VHL*$^{-/-}$ RCC Cells. Isogenic *VHL*$^{-/-}$ and *VHL*$^{+/+}$ UMRC2 cells were cultured in the presence of BPTES, BRD56491 (ROS enhancer), or their combination at the indicated

concentrations, for 72 hours. (A) Cell growth was determined by crystal violet staining and normalized to the corresponding cell type ($VHL^{-/-}$ and $VHL^{+/+}$) cultured in DMSO-containing medium. (B) Combination index values were determined using CompuSyn software. Combination index value <1 indicates drug synergy. Error bars represent SEM (n=3).

Supplementary Figure 6. Inhibition of GLS1 Selectively Impairs the Growth of *VHL*$^{-/-}$ RCC Cells. Isogenic pairs of $VHL^{-/-}$ and $VHL^{+/+}$ cells were cultured in DMSO or GLS1 inhibitors-containing medium for 72 hours and cell growth was determined by crystal violet staining. Cell growth was normalized to the corresponding cell type ($VHL^{-/-}$ or $VHL^{+/+}$) grown in DMSO-containing medium. (A-B) Effect of GLS1 inhibitor BPTES on the isogenic $VHL^{-/-}$ and $VHL^{+/+}$ RCC4 (A), and UOK102 (B) cells. (C-E) Effect of GLS1 inhibitor CB-839 on the isogenic $VHL^{-/-}$ and $VHL^{+/+}$ RCC4 (C), and UOK102 (D) cells, and the corresponding GI50 concentrations (E). Error bars represent SEM (n=3). *P < 0.05, **P < 0.01, ***P < 0.001, Student's *t*-test between $VHL^{-/-}$ and $VHL^{+/+}$ cells.

Supplementary Figure 7. Administration of Exogenous Metabolites Can Rescue the Growth Inhibitory Effect of GLS1 Inhibitors on *VHL*$^{-/-}$ Cells in All Tested Cell Lines. Isogenic $VHL^{-/-}$ and $VHL^{+/+}$ RCC4 (A-D) and UOK102 (E-H) cells were treated with BPTES in the presence or absence of exogenous glutamate (2 mM), dimethyl alpha-ketoglutarate (DM-αKG) (0.5 mM), nucleobases (5 μM), or N-acetyl cysteine (NAC) (4 mM). Relative cell growth was determined by crystal violet staining and normalized to the growth of DMSO treated cells when supplemented with the corresponding metabolite. Error bars represent SEM (n=3). *P < 0.05, ***P < 0.001, Student's *t*-test compares the effect of exogenous metabolites on the growth of cells.

Supplementary Figure 8. GLS1 Inhibitor BPTES Induces DNA Replication Stress in *VHL*$^{-/-}$ RCC4 Cells. Isogenic $VHL^{-/-}$ and $VHL^{+/+}$ RCC4 cell were treated with 1.5 μM BPTES for 24 hours, in the presence or absence of 1 mM glutamate or 0.5 mM dimethyl alpha-ketoglutarate (DM-αKG). EdU incorporation and PI staining were quantified by FACS analysis. Flow cytometry dot plots of $VHL^{-/-}$ (A) and $VHL^{+/+}$ (B) RCC4 cells are presented. Treatment with BPTES did not alter the cell cycle distribution of $VHL^{-/-}$ (C) or $VHL^{+/+}$ (D) RCC4 cells but

significantly altered the DNA synthesis of *VHL*$^{-/-}$ cells compared to their isogenic *VHL*$^{+/+}$ counterparts (E). (A-E) Addition of glutamate or DM-αKG in the tissue culture medium restored DNA synthesis in *VHL*$^{-/-}$ cells to levels comparable to *VHL*$^{+/+}$ cells.

Supplementary Figure 9. Time-dependent Effect of GLS1 Inhibitor BPTES on DNA Synthesis of *VHL*$^{-/-}$ UMRC2 Cells. Isogenic *VHL*$^{-/-}$ (A, C and E) and *VHL*$^{+/+}$ (B, D and F) UMRC2 cells were treated with DMSO vehicle control (A and B), 1.5 μM BPTES (C and D), or 1.5 μM BPTES in the presence of 0.5 mM dimethyl alpha-ketoglutarate (DM-αKG) (E and F) for 72 hours. (A-F) DNA synthesis was quantified by pulse EdU incorporation at 24, 48 and 72 hours of treatment. (G) Suppression of DNA synthesis by BPTES at the indicated time points.

Supplementary Figure 10. Detection of DNA Replication Stress by Single Strand Sensors phospho-CHK1 and RPA32. Isogenic *VHL*$^{-/-}$ and *VHL*$^{+/+}$ UMRC2 cells were treated with the indicated concentrations of GLS1 inhibitors BPTES, CB-839 for 48 hours or 2 mM hydroxyurea (HU) for 16 hours. Total amount and phosphsorylated species of DNA replication stress sensors CHK1 and RPA32 were resolved in SDS-PAGE gel and detected by immunoblot. Treatment with HU, but not with GLS1 inhibitors, resulted in detectable phosphorylation of CHK1 and RPA32.

Supplementary Figure 11. Low Concentration of Hydroxyurea Selectively Induces DNA Replication Stress in *VHL*$^{-/-}$ RCC Cells. Isogenic *VHL*$^{-/-}$ and *VHL*$^{+/+}$ UMRC2 cell were cultured in the presence or absence of hydroxyurea. (A-D) DNA synthesis rate of *VHL*$^{-/-}$ and *VHL*$^{+/+}$ UMRC2 cells was quantified by EdU incorporation. Representative flow cytometry dot plots of *VHL*$^{-/-}$ (A) and *VHL*$^{+/+}$ (B) UMRC2 cells. Cell cycle distribution of *VHL*$^{-/-}$ (C) and *VHL*$^{+/+}$ (D) UMRC2 cells. (E) Total amount and phosphsorylated species of a DNA replication stress sensor CHK1 was resolved in SDS-PAGE gel and detected by immunoblot. (F) Cell growth was determined by crystal violet staining and normalized to the corresponding cell type (*VHL*$^{-/-}$ and *VHL*$^{+/+}$) cultured in DMSO-containing medium. Error bars represent SEM (n=3). **P < 0.01, ***P < 0.001, Dunnett's test against DMSO treated cells.

Supplementary Figure 12. ROS Enhancement Synergizes with GLS1 Inhibitors to Enhance DNA Replication Stress in *VHL*$^{-/-}$ RCC Cells. Isogenic *VHL*$^{-/-}$ and *VHL*$^{+/+}$ UMRC2 cells were

cultured in the presence or absence of 0.5 μM BPTES or 2.5 μM BRD56491 (ROS enhancer), or their combination. (A-C) DNA synthesis rate of *VHL*$^{-/-}$ and *VHL*$^{+/+}$ UMRC2 cells was quantified by EdU incorporation. Representative flow cytometry dot plots of *VHL*$^{-/-}$ (A) and *VHL*$^{+/+}$ (B) UMRC2 cells. (C) Percentage of LOW EdU incorporating cells (% cells in DNA replication stress). (D) Percentage of nuclei with the indicated number of γH2AX foci after the treatment. (E) BRD56491 synergistically enhanced intracellular ROS levels with BPTES in *VHL*$^{-/-}$ UMRC2 cells. Error bars represent SEM (n=3). **P < 0.01, ***P < 0.001, Dunnett's test against DMSO treated cells.

Supplementary Figures 13. **Synergistic Effect of PARP Inhibitor Olaparib with GLS1 Inhibitors on Growth Suppression of *VHL*$^{-/-}$ RCC Cells.**
Isogenic *VHL*$^{-/-}$ and *VHL*$^{+/+}$ UMRC2 (Figure A-B), RCC4 (Figure C-D) and UOK102 (E-H) were cultured in the presence of GLS1 inhibitors BPTES or CB-839 (as indicated) alone or in combination with the PARP inhibitor olaparib, at the indicated concentrations, for 72 hours. Cell growth is normalized to treatment with DMSO vehicle control (relative cell growth in A, C, E, and G). Combination index values were determined using CompuSyn software (B, D, F, and H). Combination index value <1 indicates drug synergy. Error bars represent SEM (n=3).

Supplementary Figure 14. PARP Inhibition Synergizes with GLS1 Inhibitors to Suppress the Growth of *VHL*$^{-/-}$ RCC Cells *in vitro* and *in vivo*. (A) UMRC3 cells were cultured in the absence or presence of CB-839 and olaparib, at the indicated concentrations, for 72 hours. *In vitro* cell growth was determined by crystal violet staining and normalized to the DMSO control. (B) Combination index values were determined using CompuSyn software. Combination index value <1 indicates drug synergy. (C-H) UMRC3 xenografts were treated with vehicle control, CB-839 (200 mg/kg, twice daily), olaparib (75 mg/kg. once daily), or the combination of CB-839 and olaparib. Body weight change (C), tumor weight at the experimental endpoint (D), growth of individual tumors of vehicle (E), CB-839 (F), olaparib (G), and the combination (H) are shown.

Supplementary Figure 15. HIF-2α Expression is Sufficient to Confer Sensitivity to GLS1 Inhibition in Combination with Olaparib. *VHL*-replete 786-O cells were stably infected with retroviral vectors expressing the *VHL*-resistant HIF-2α (P405toA/P531toA) mutant or empty

vector as control. (A) Cells were treated with increasing concentrations of CB-839, olaparib or their combination as indicated. (B) Western blot confirming the expression of *VHL* and HIF-2α (P405toA/P531toA) mutant in the engineered cell lines.

Supplementary Figure 16. PARP Inhibition Synergizes with GLS1 Inhibitors to Suppress Proliferation of *VHL*$^{-/-}$ RCC Cells as Mouse Xenografts. (A) Tumors of UMRC3 xenografts treated with vehicle control, CB-839, olaparib, or their combination (as indicated) were scored for proliferation (Ki-67) or apoptosis (TUNEL). H&E indicates tumor staining with hematoxylin and eosin. (B) Quantification of xenograft Ki-67 for each treatment arm (n=9; analysis of 3 tumors x 3 random areas of Ki-67 quantification per tumor). *P < 0.05, **P < 0.01, comparison of indicated arm to vehicle treatment control.

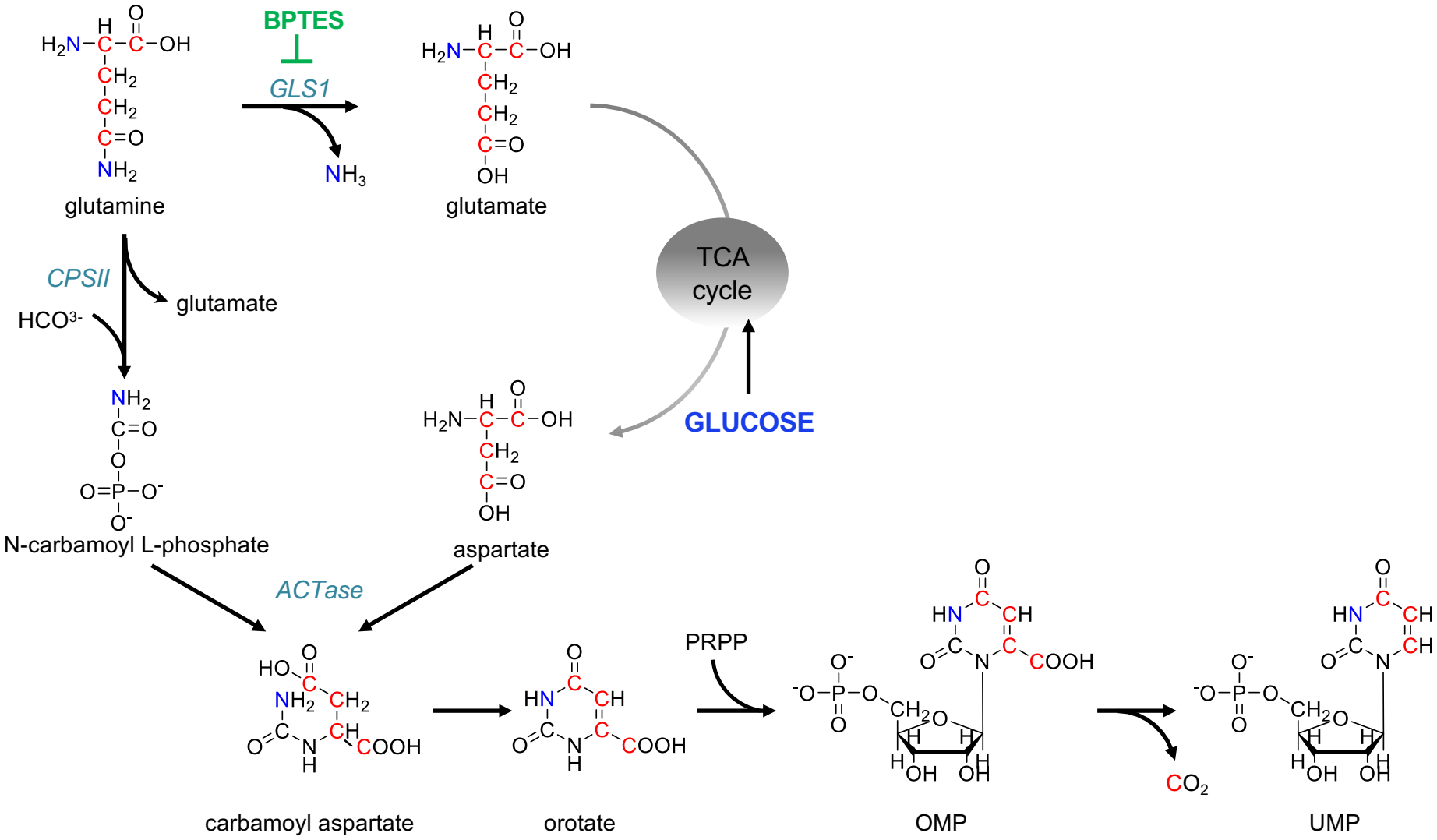

Supplementary Figure 1

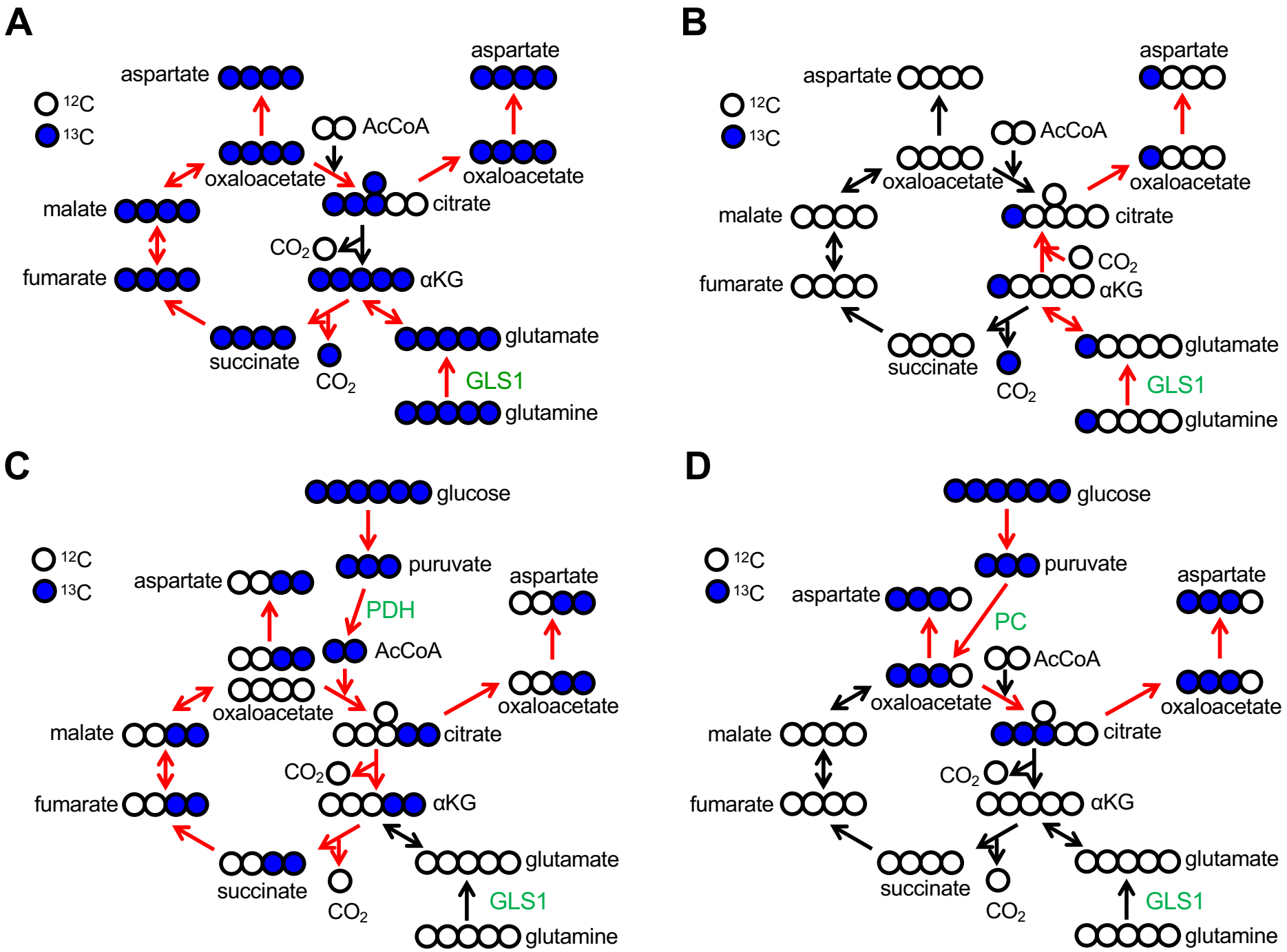

Supplementary Figure 2

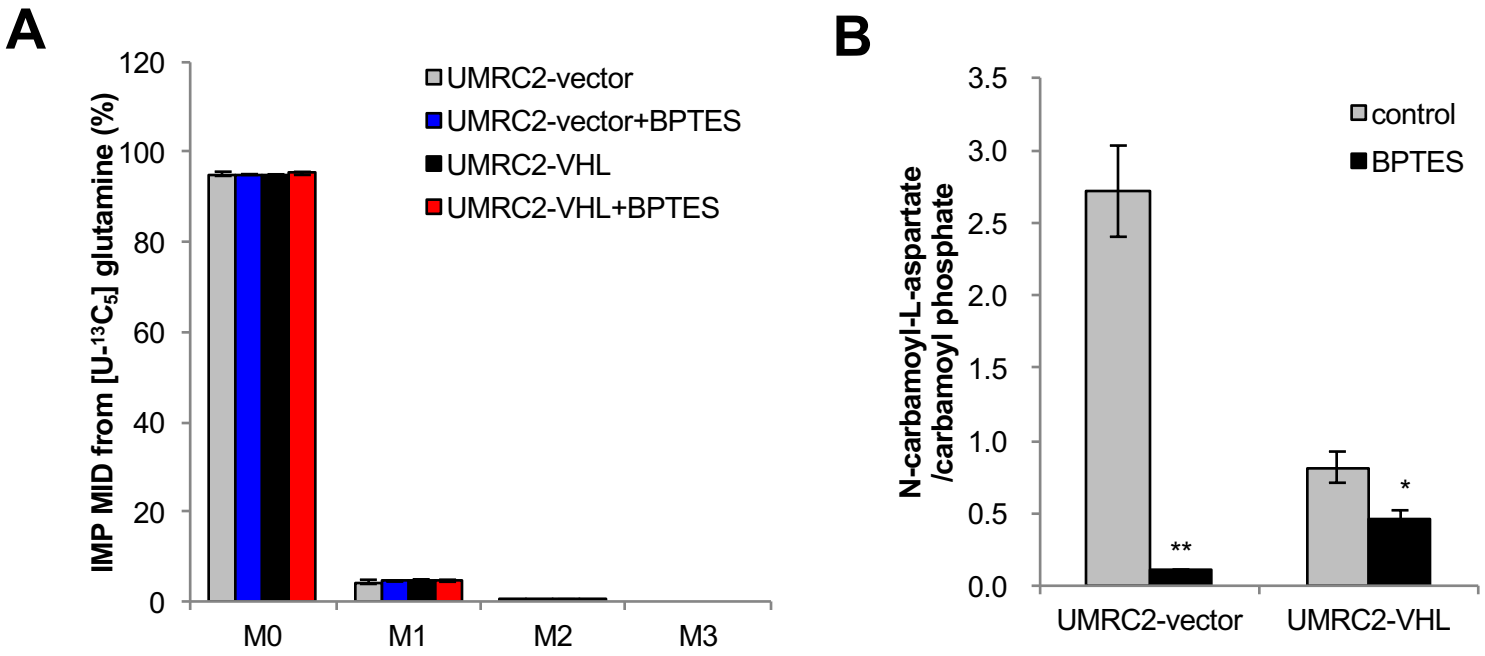

Supplementary Figure 3

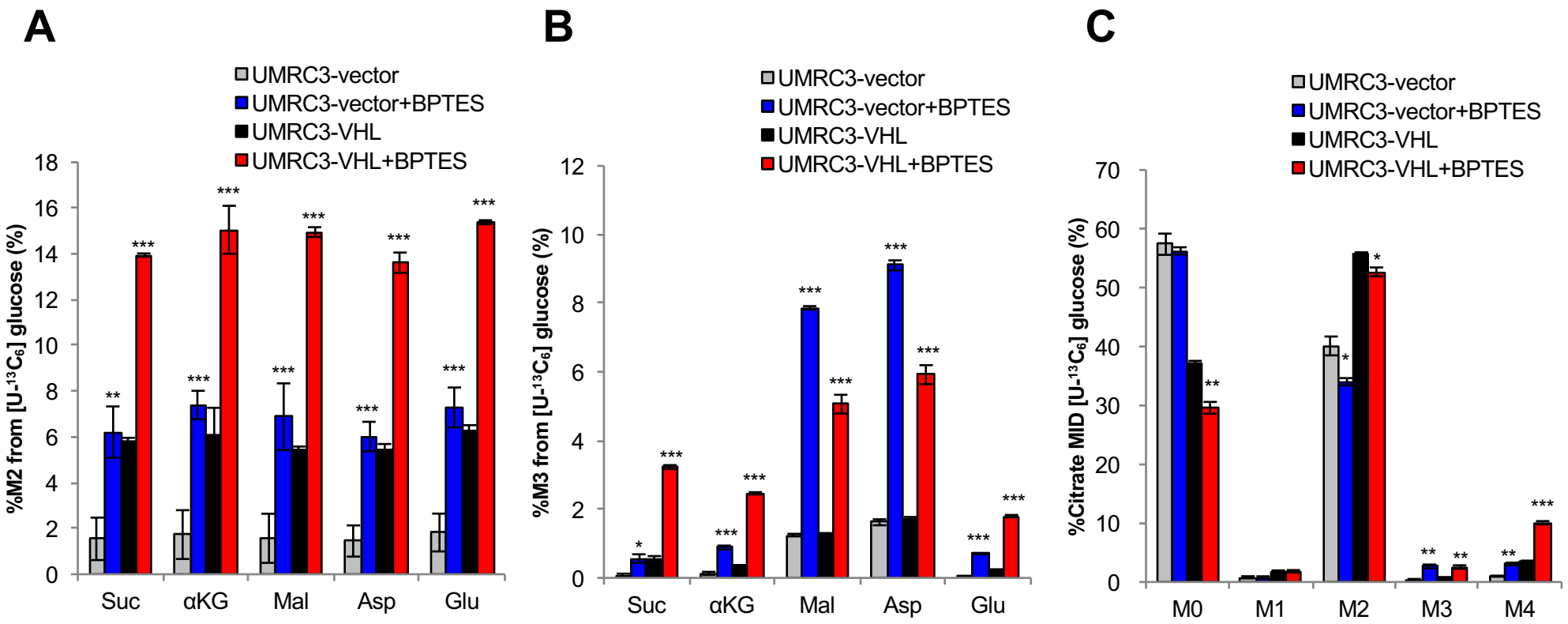

Supplementary Figure 4

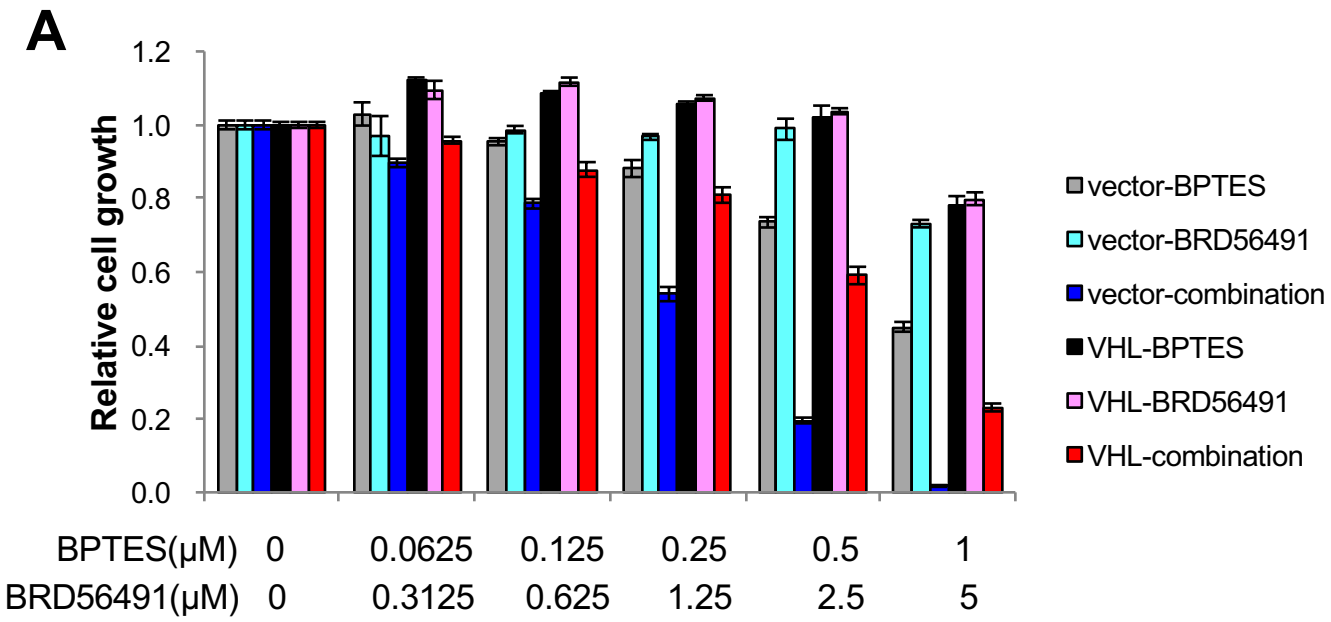

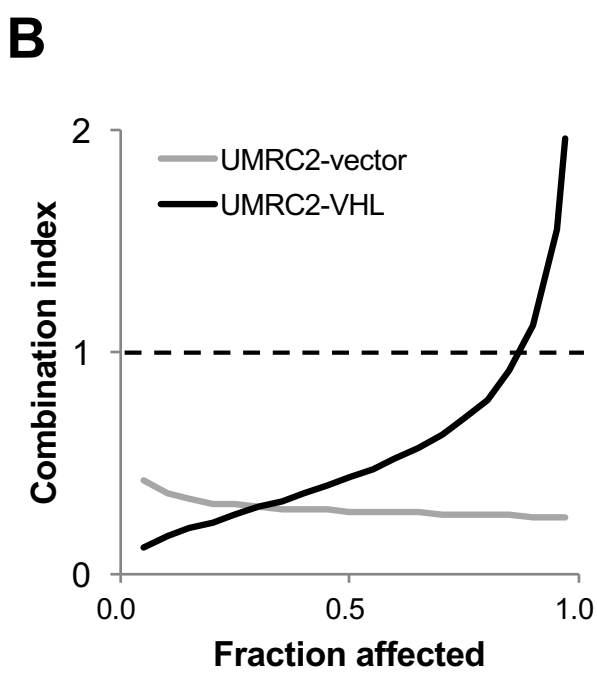

Supplementary Figure 5

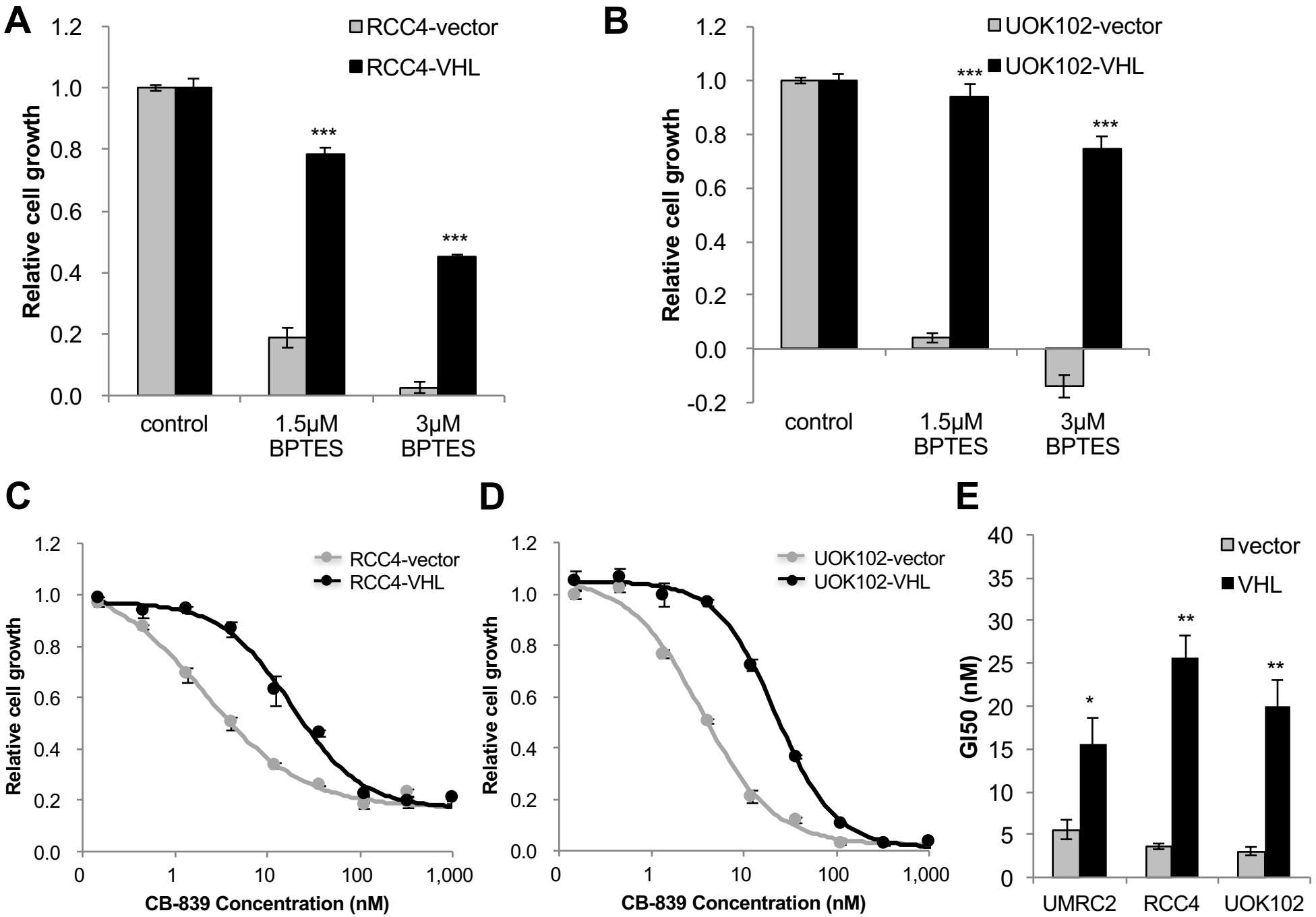

Supplementary Figure 6

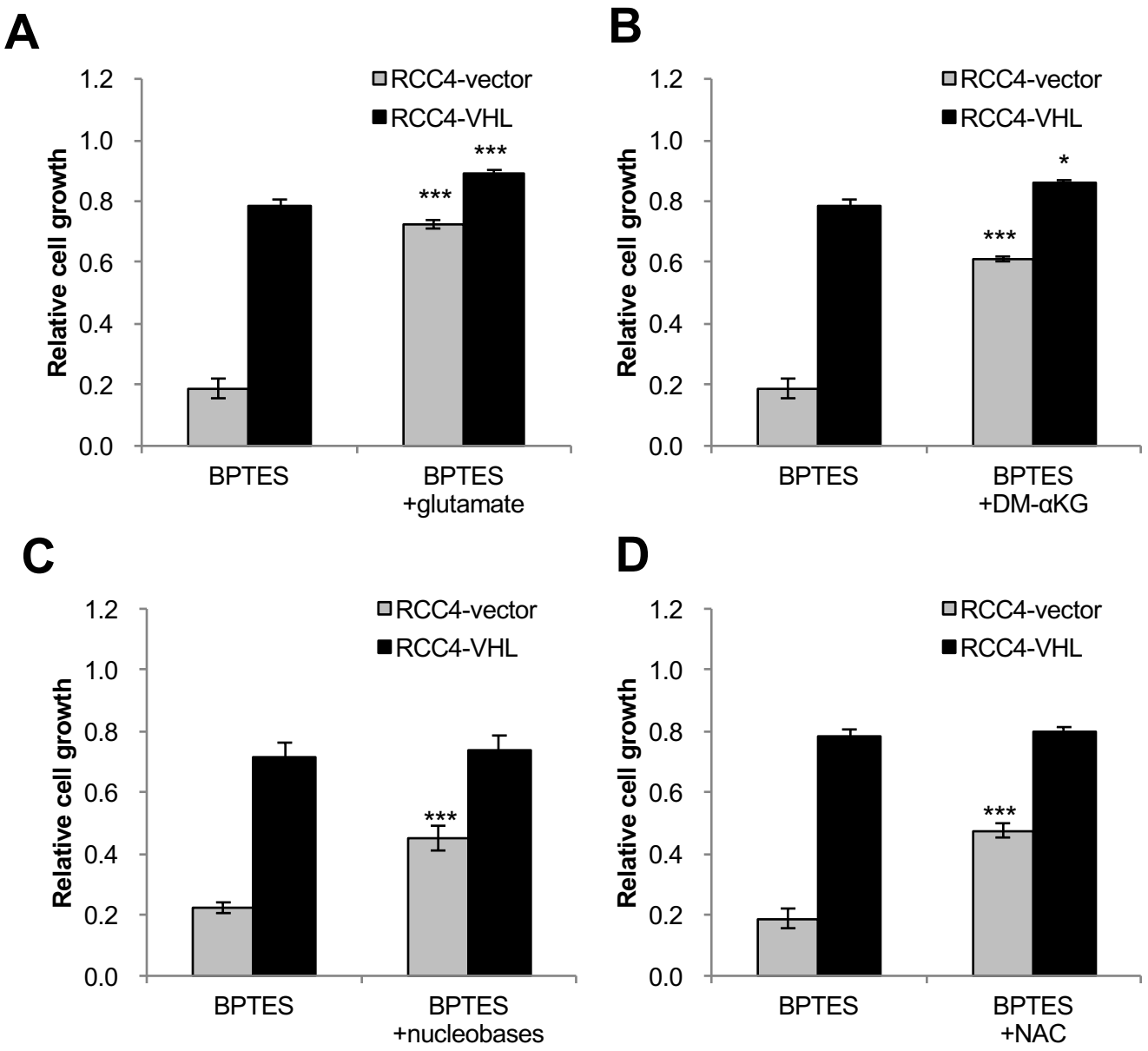

Supplementary Figure 7

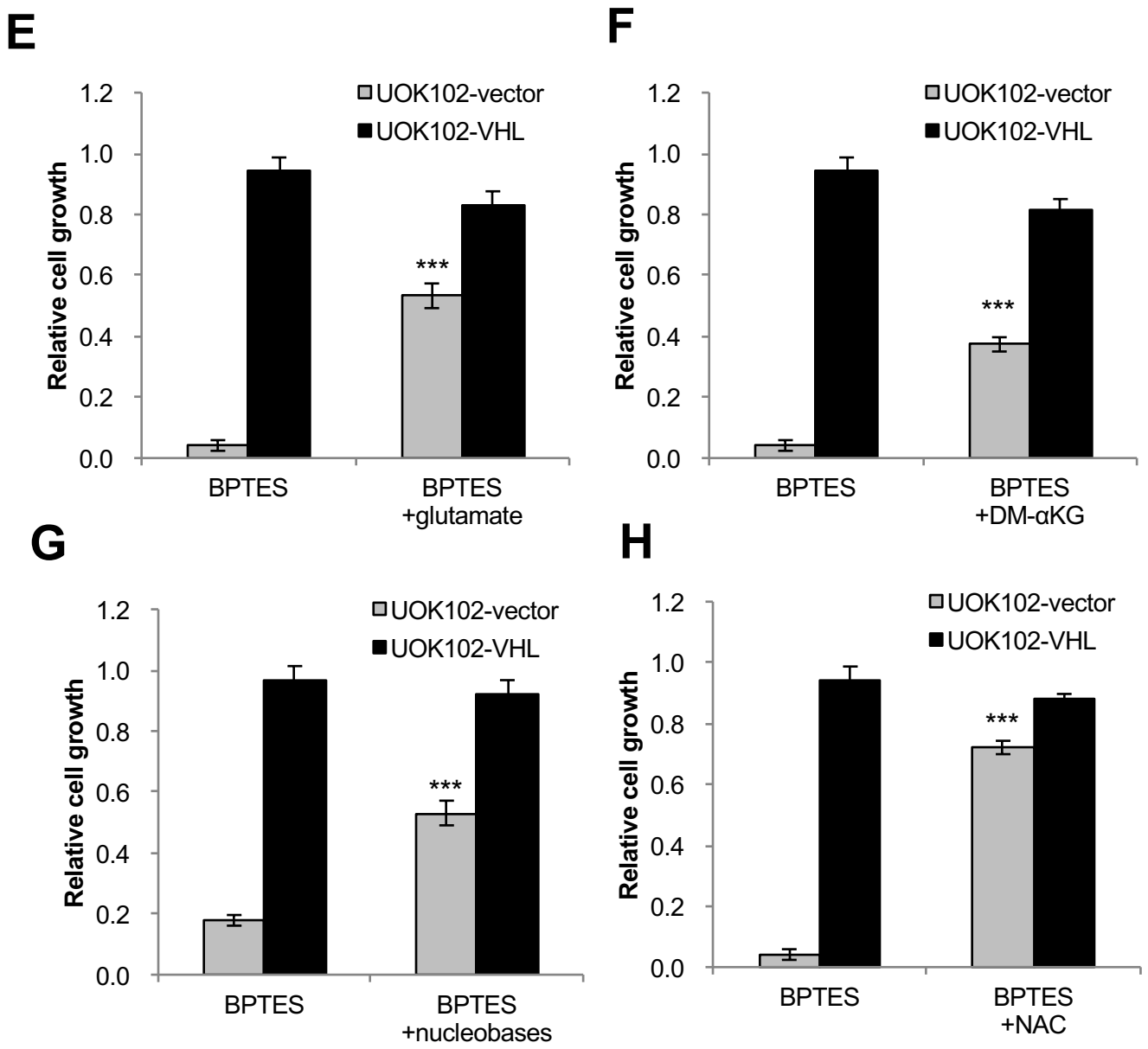

Supplementary Figure 7

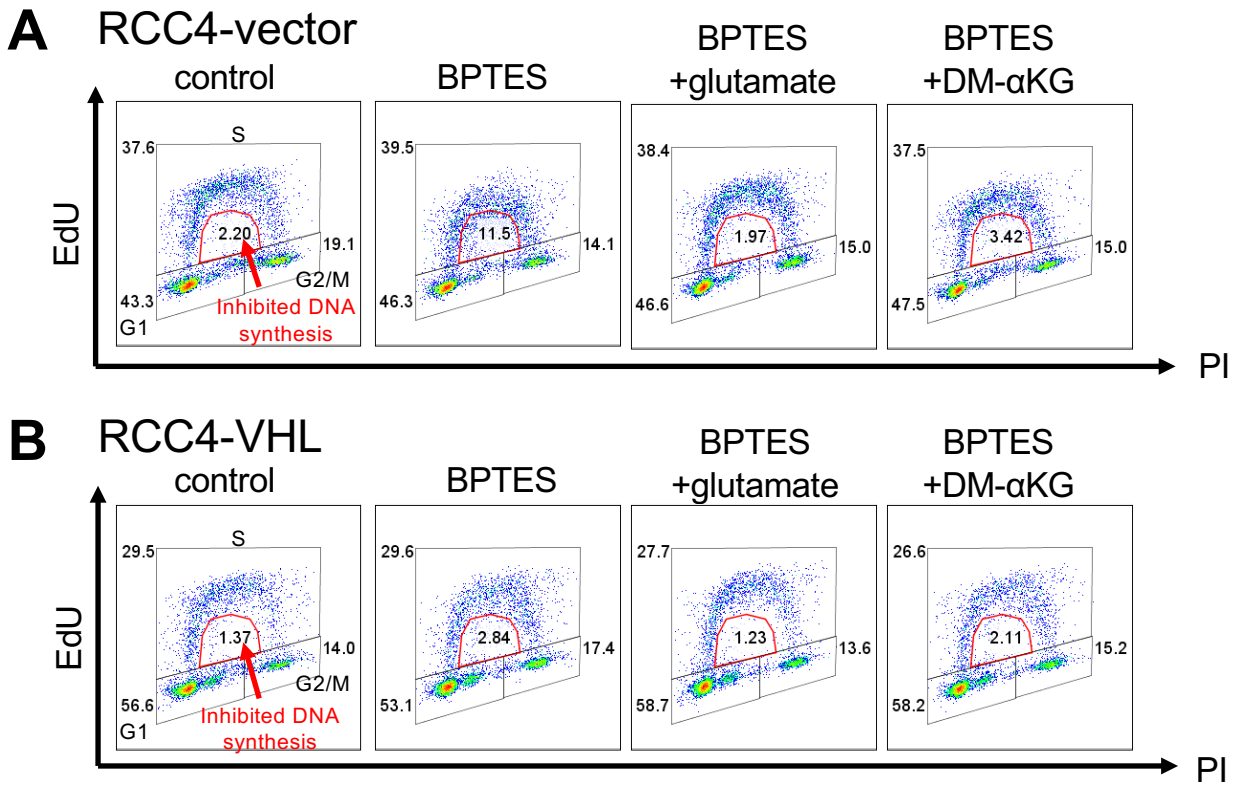

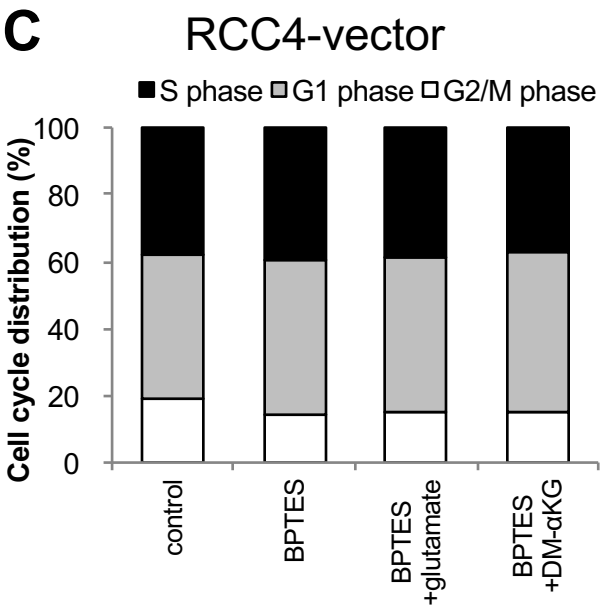

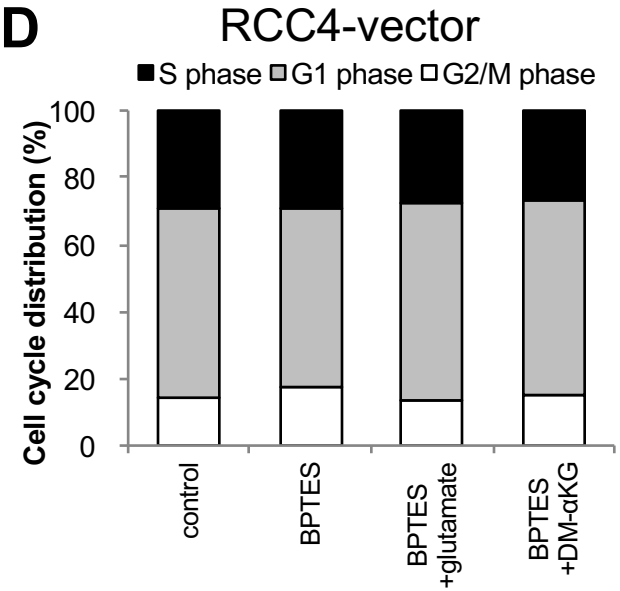

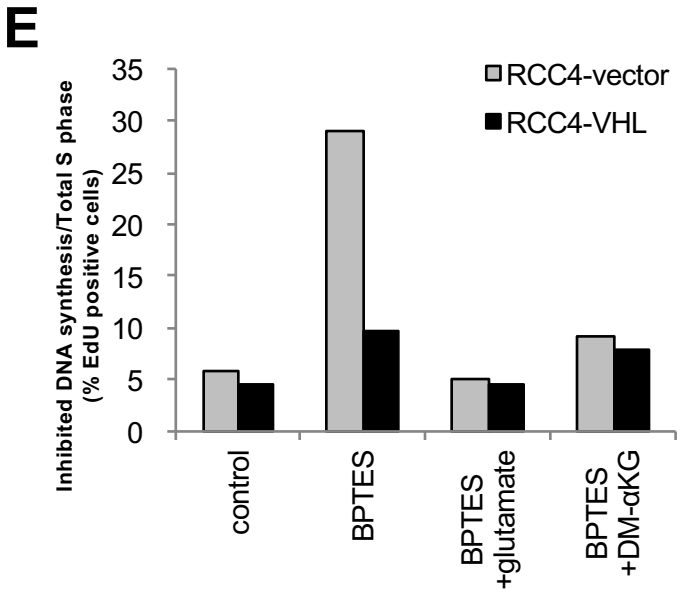

Supplementary Figure 8

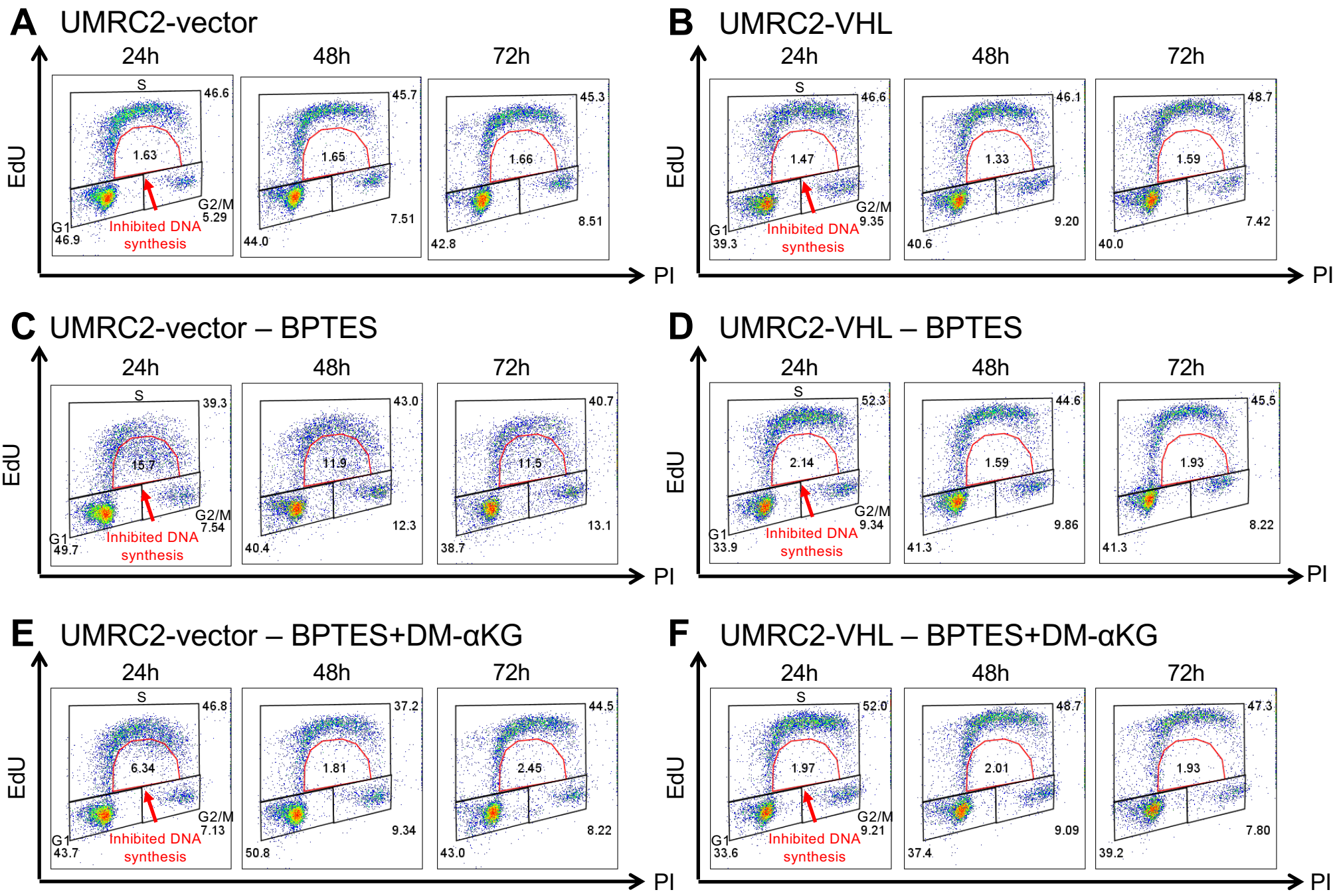

Supplementary Figure 9

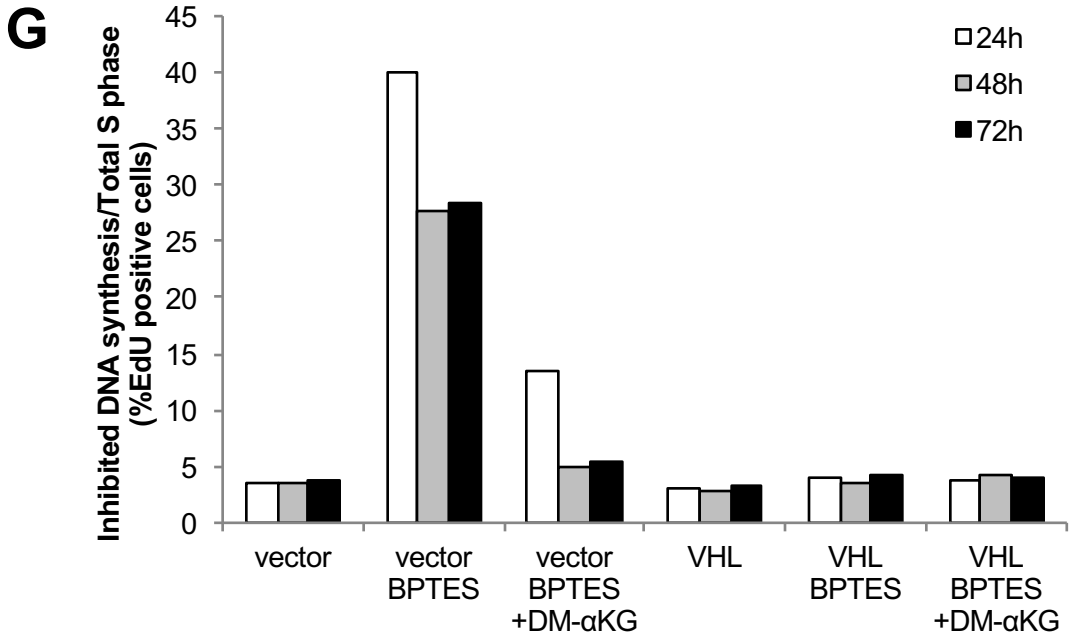

Supplementary Figure 9

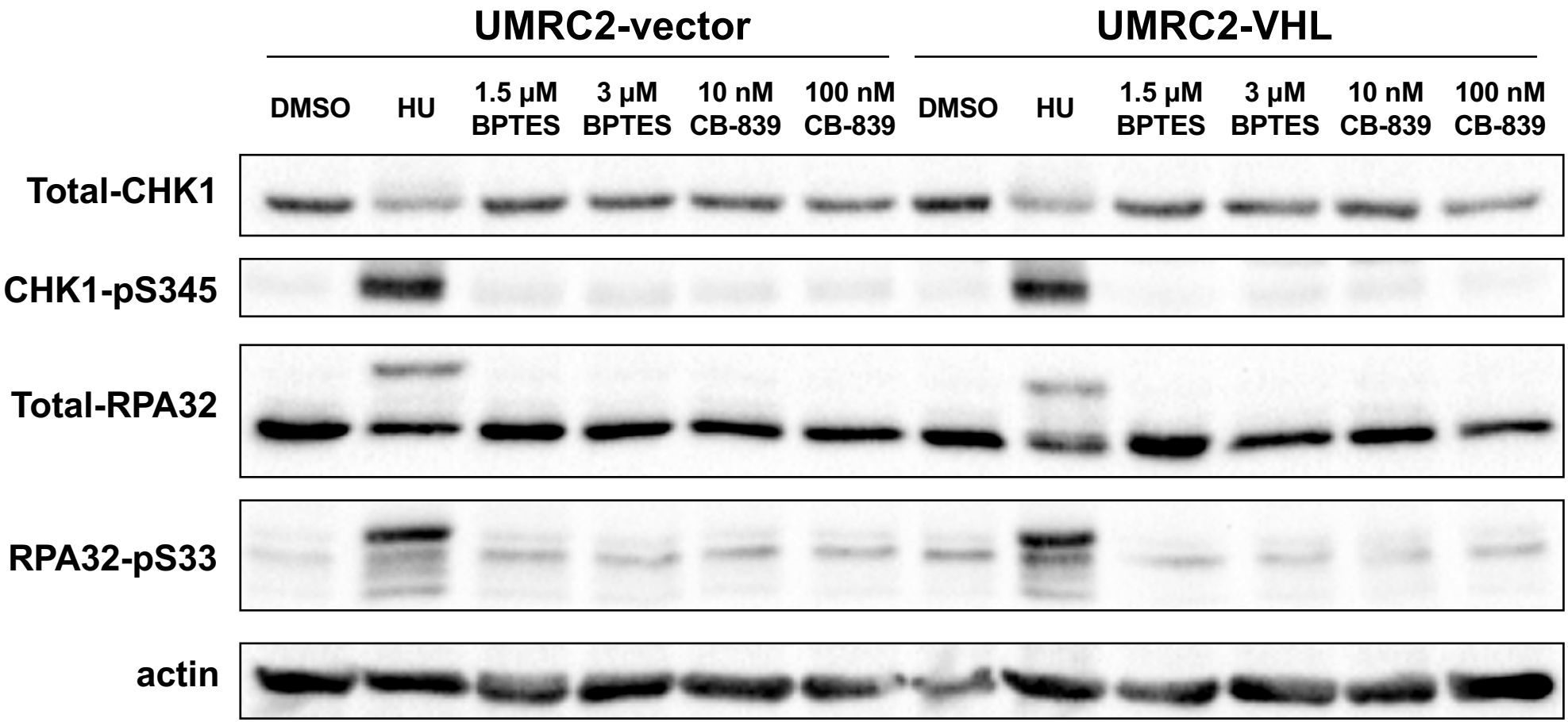

Supplementary Figure 10

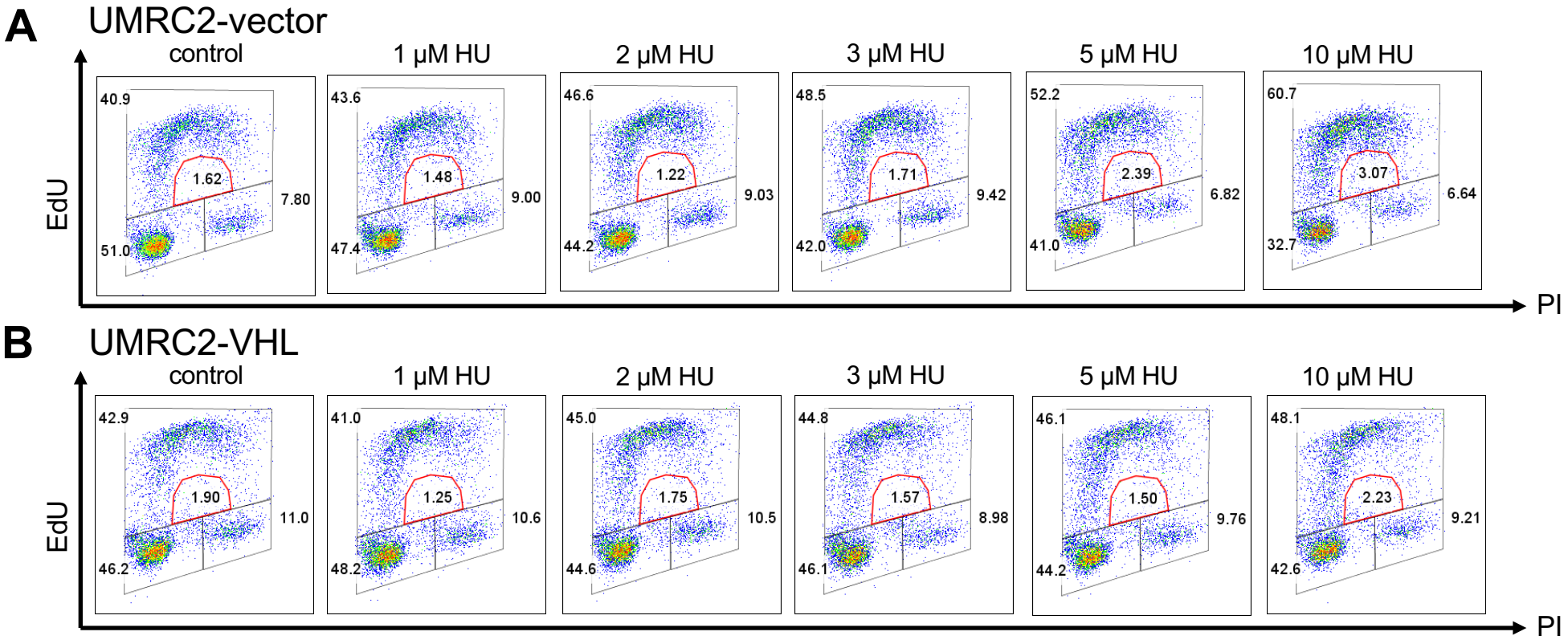

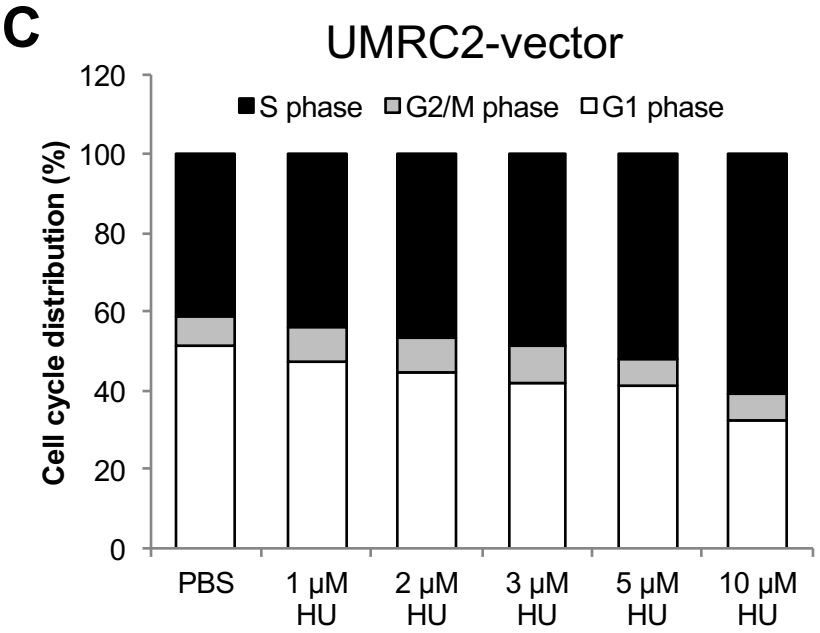

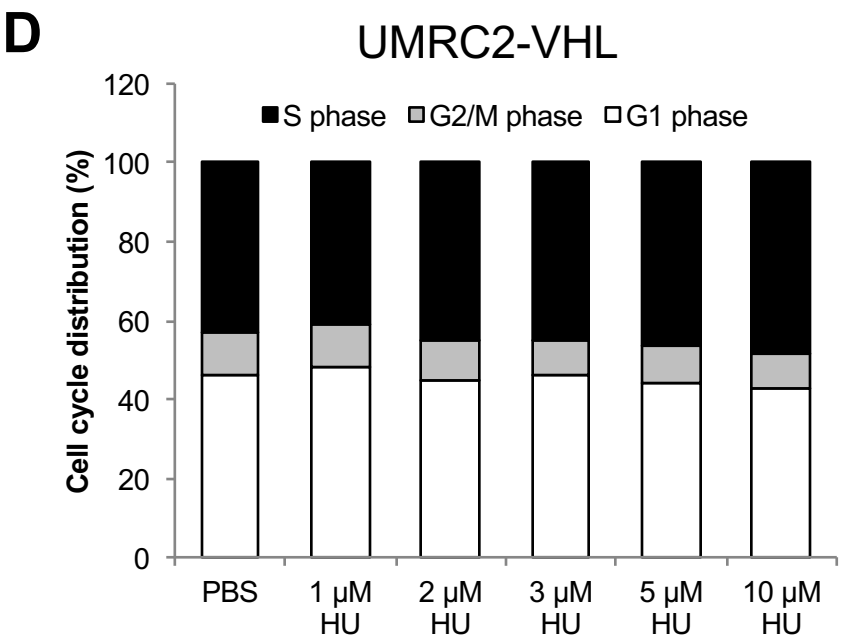

Supplementary Figure 11

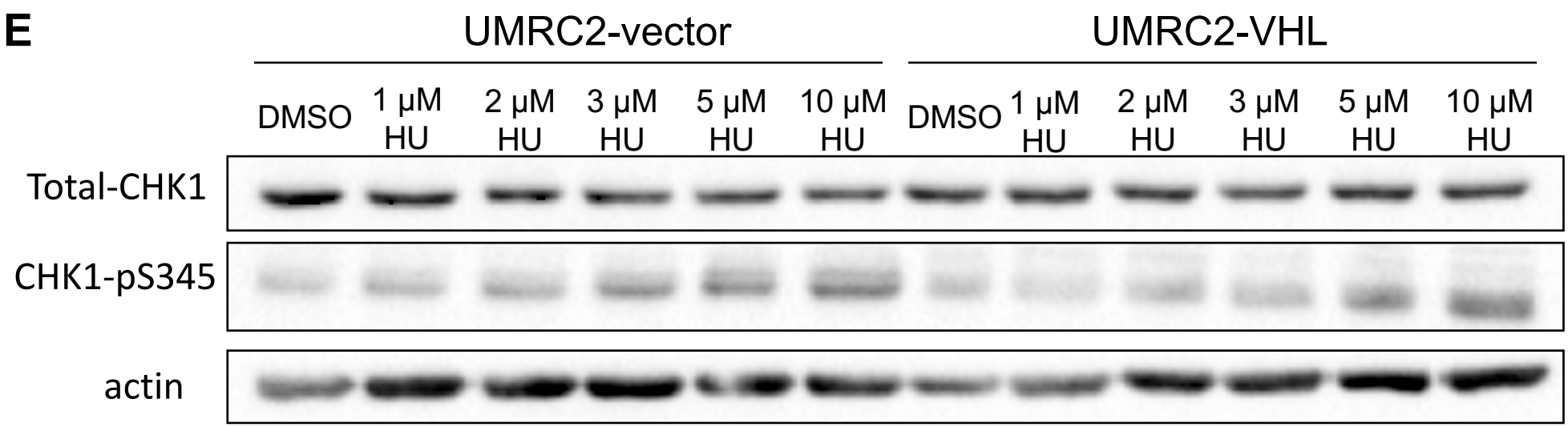

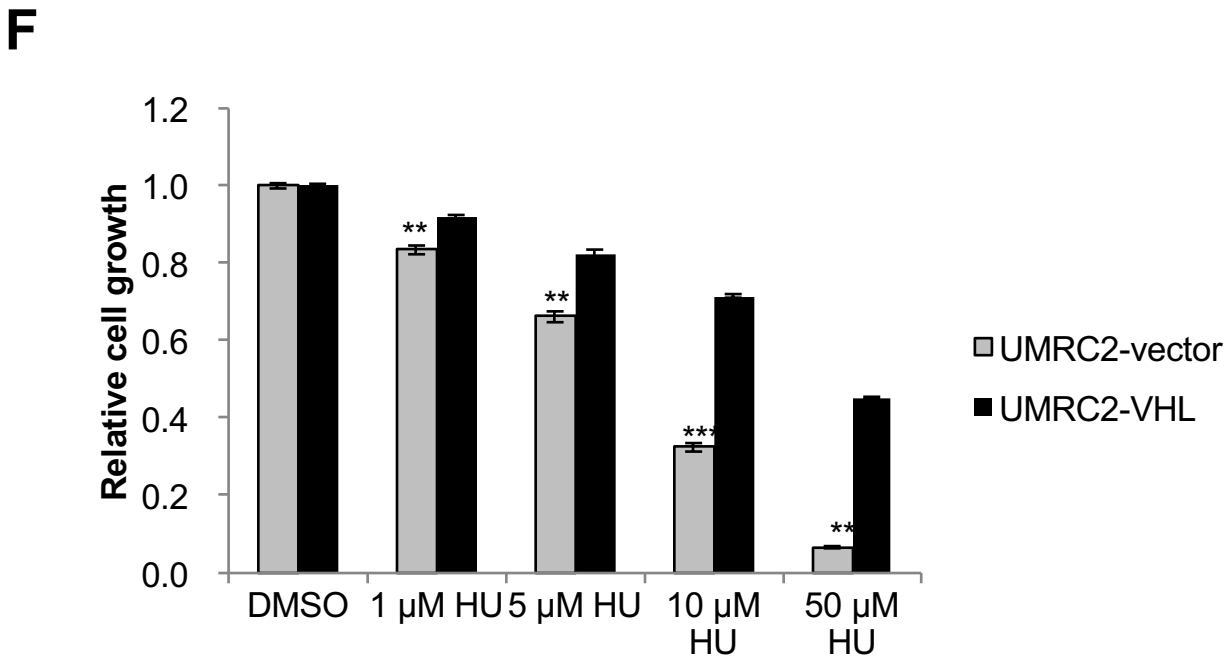

Supplementary Figure 11

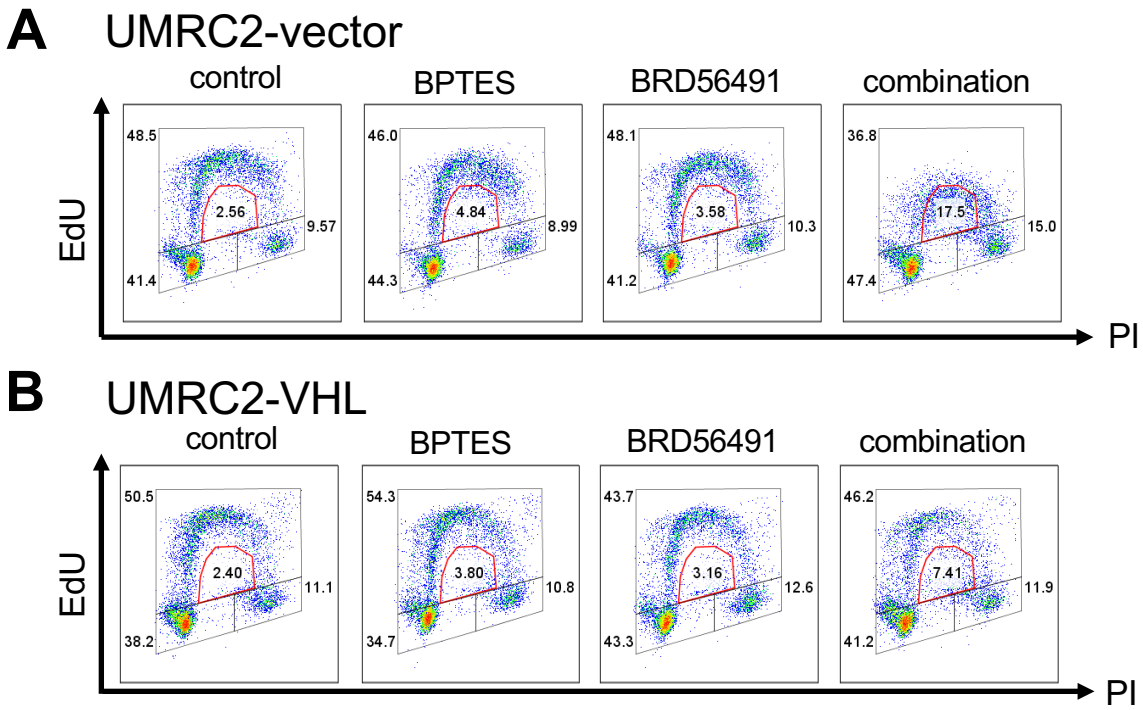

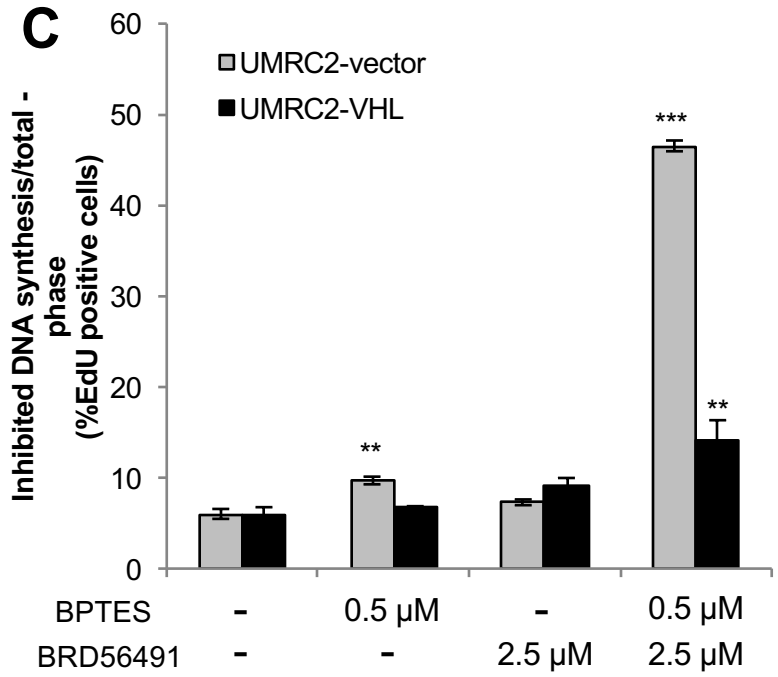

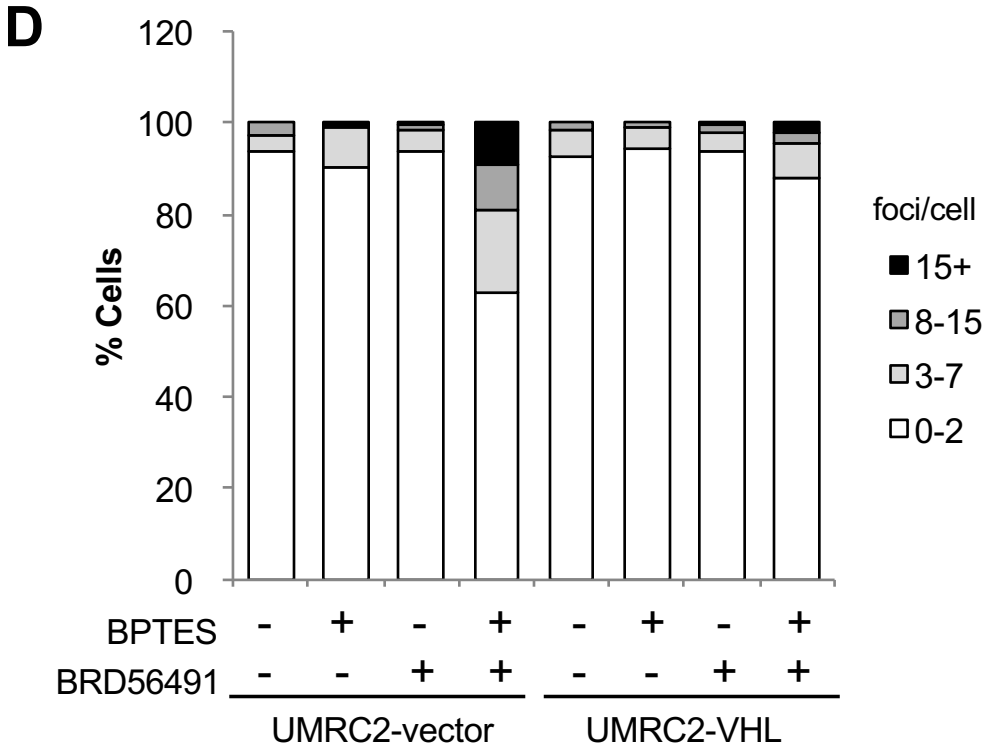

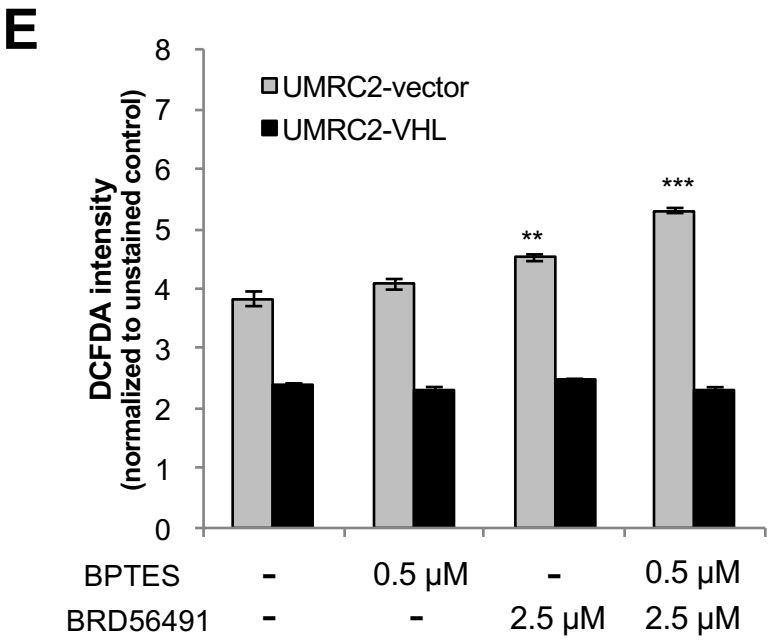

Supplementary Figure 12

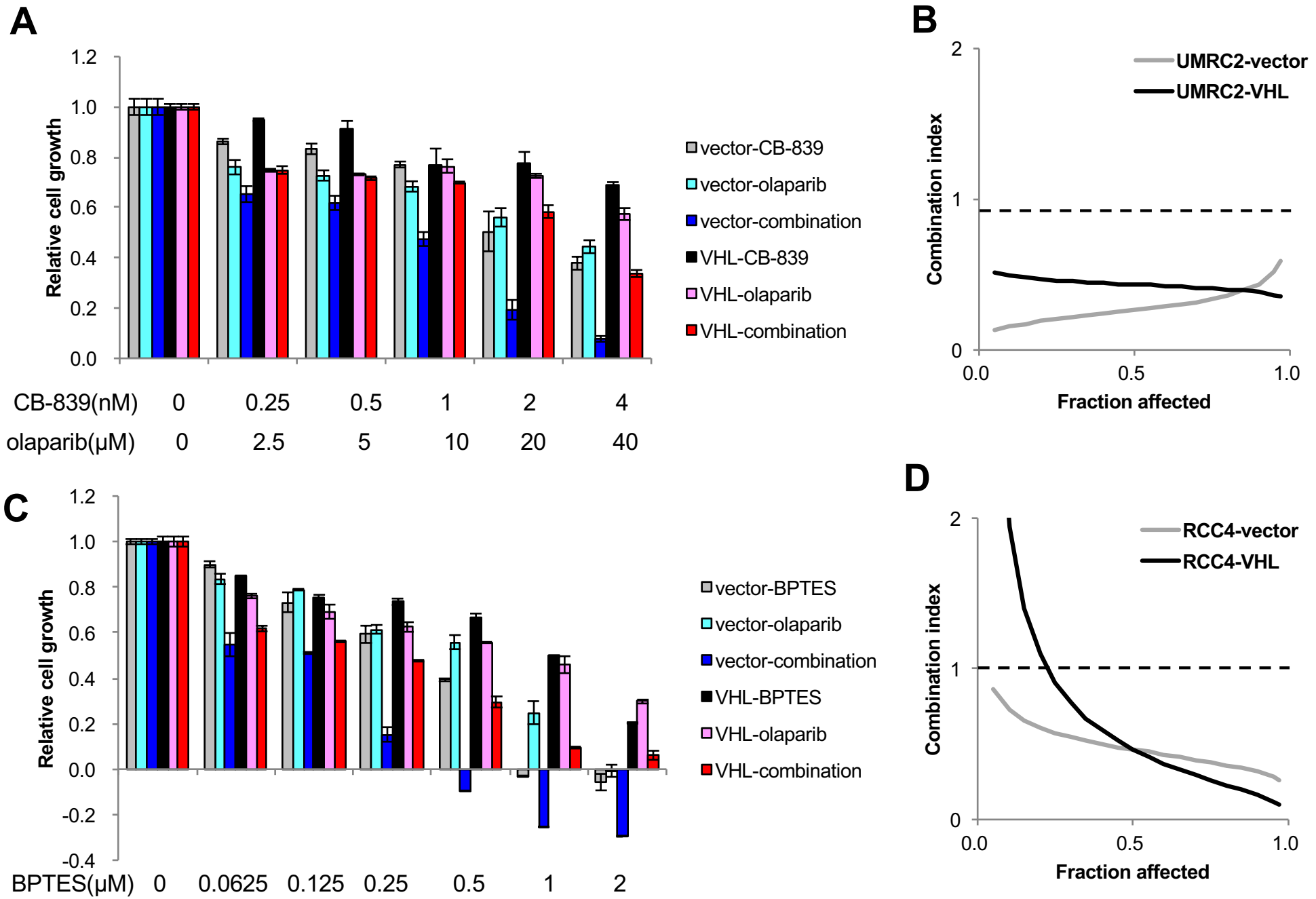

Supplementary Figure 13

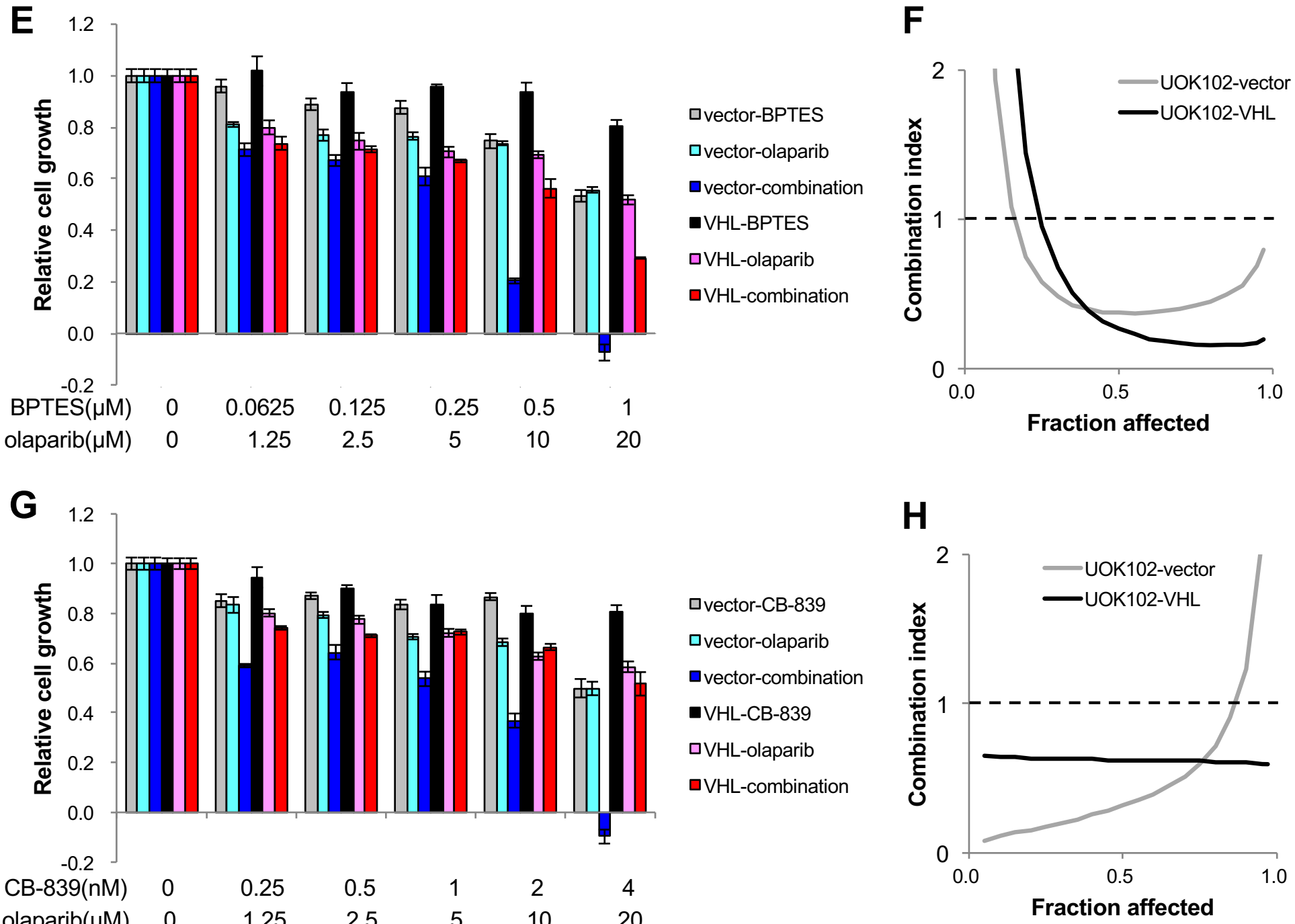

Supplementary Figure 13

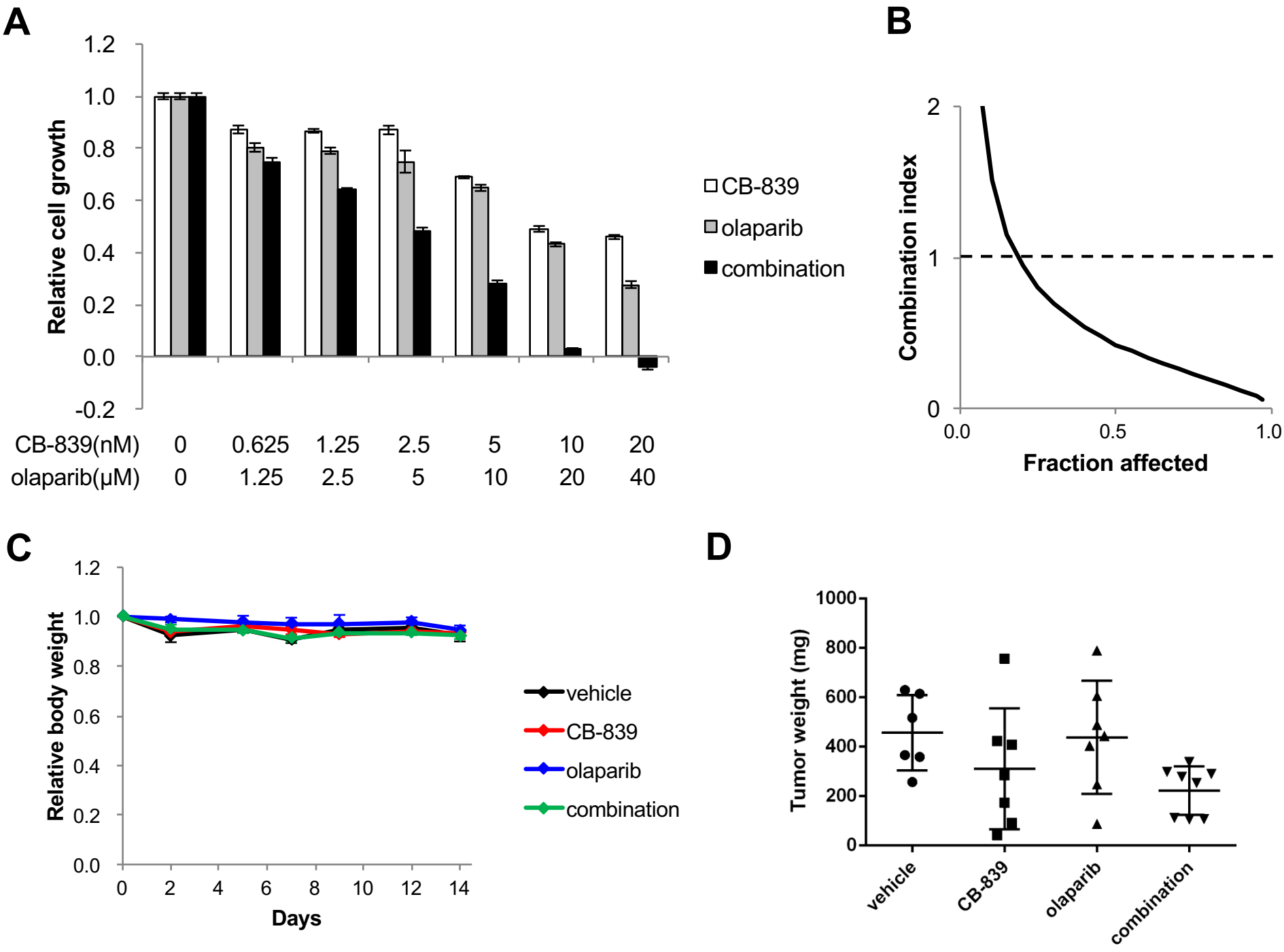

Supplementary Figure 14

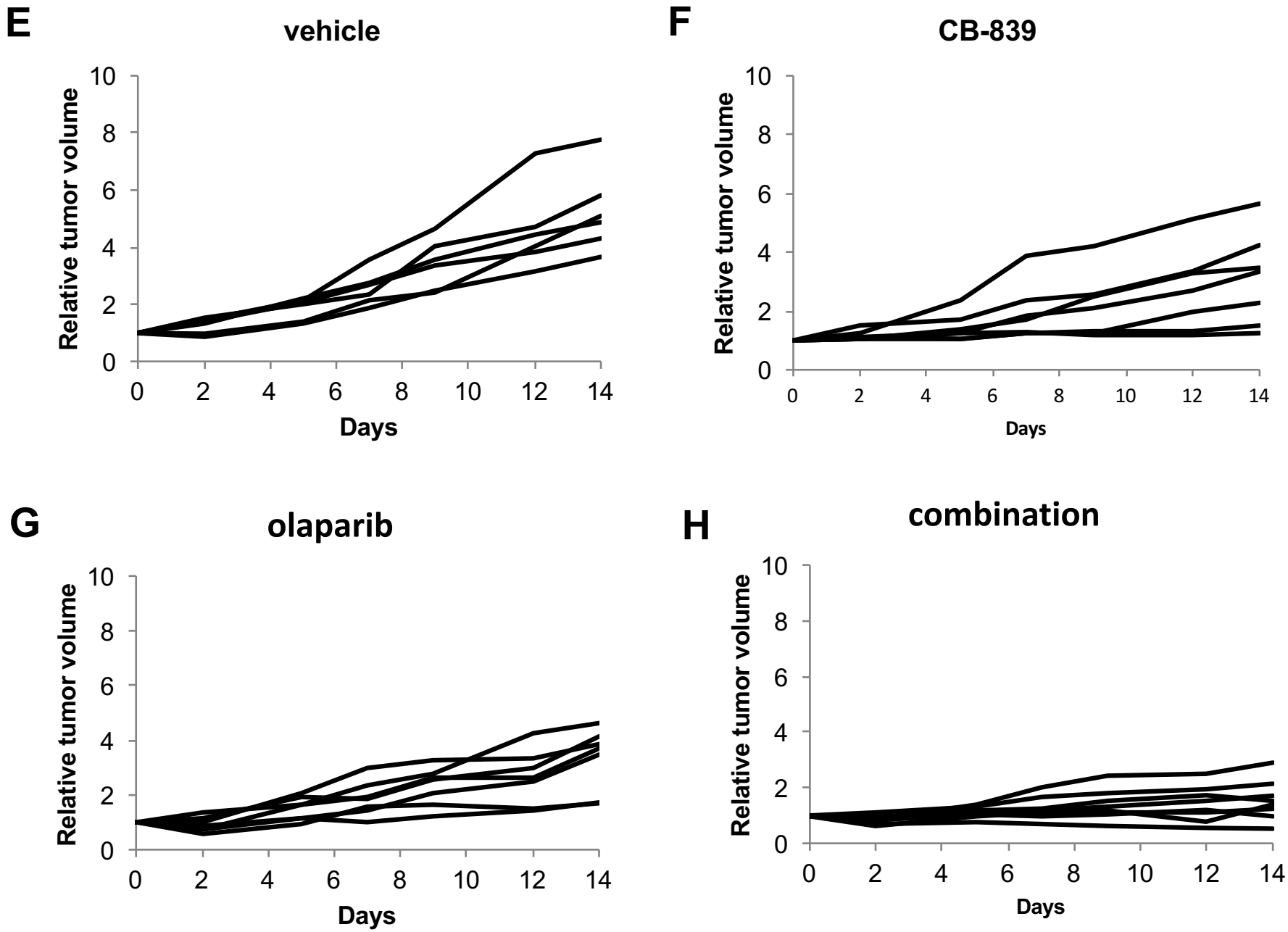

Supplementary Figure 14

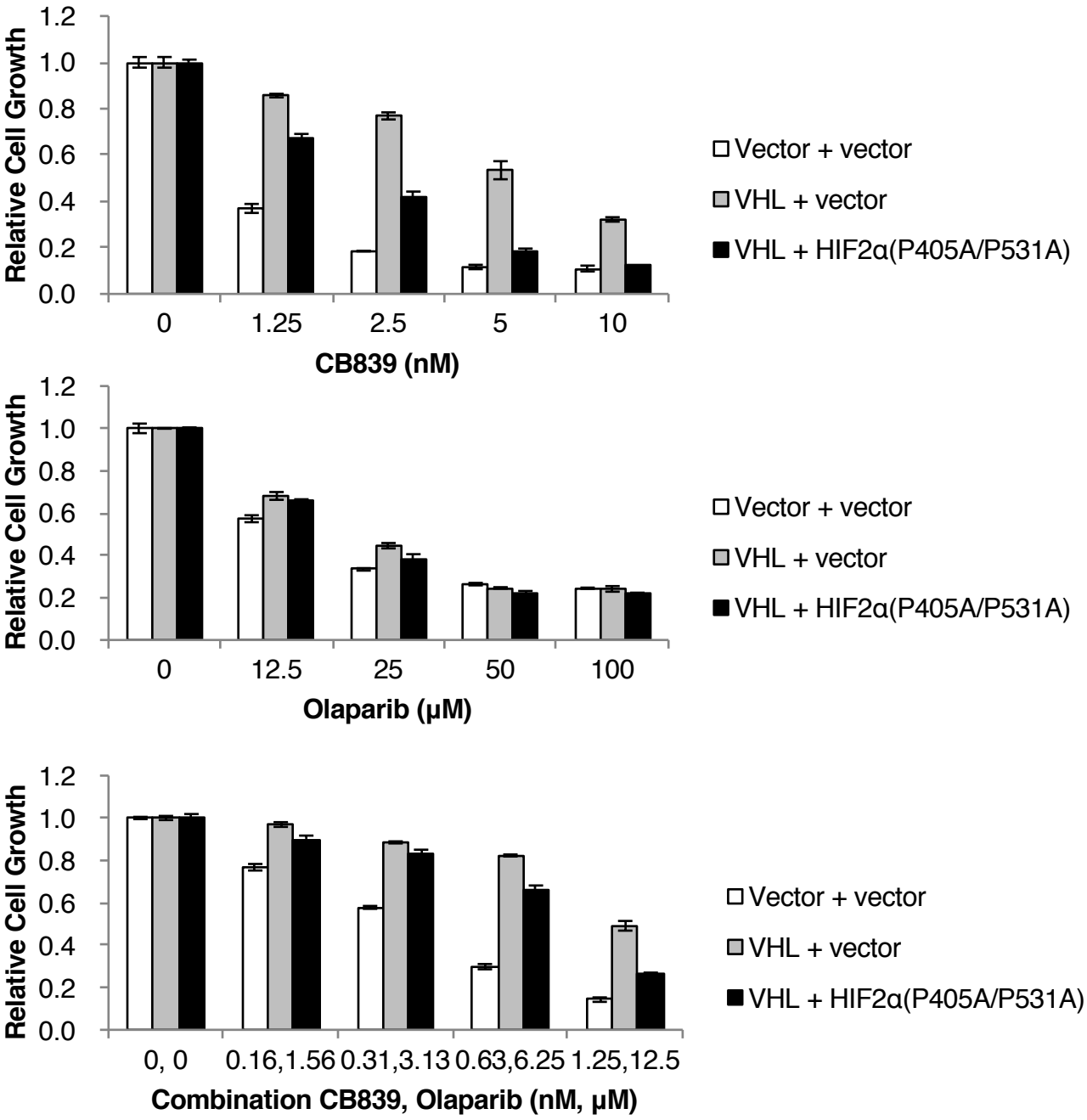

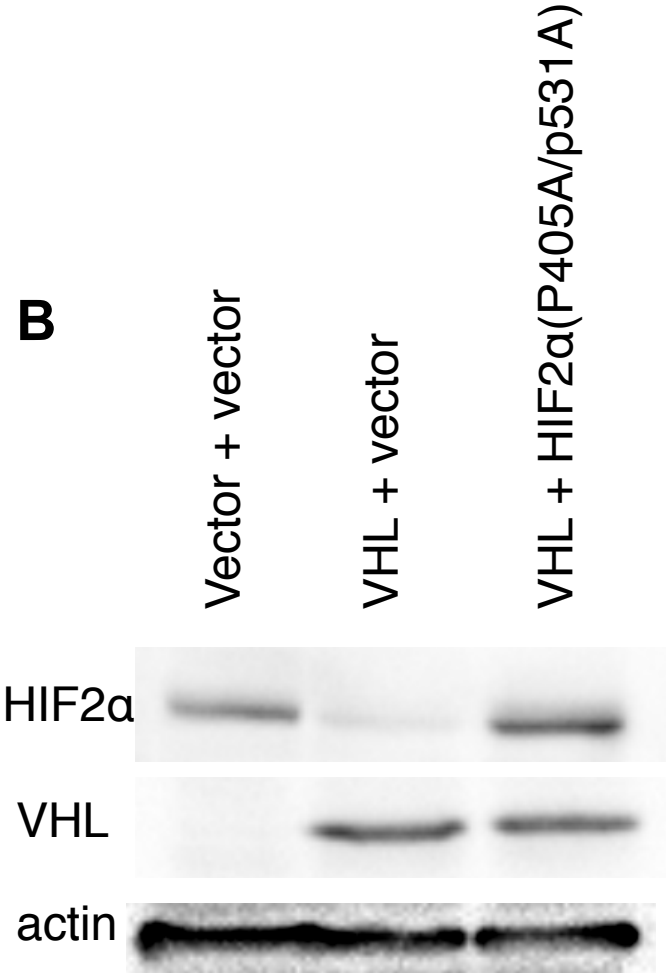

Supplementary Figure 15

A

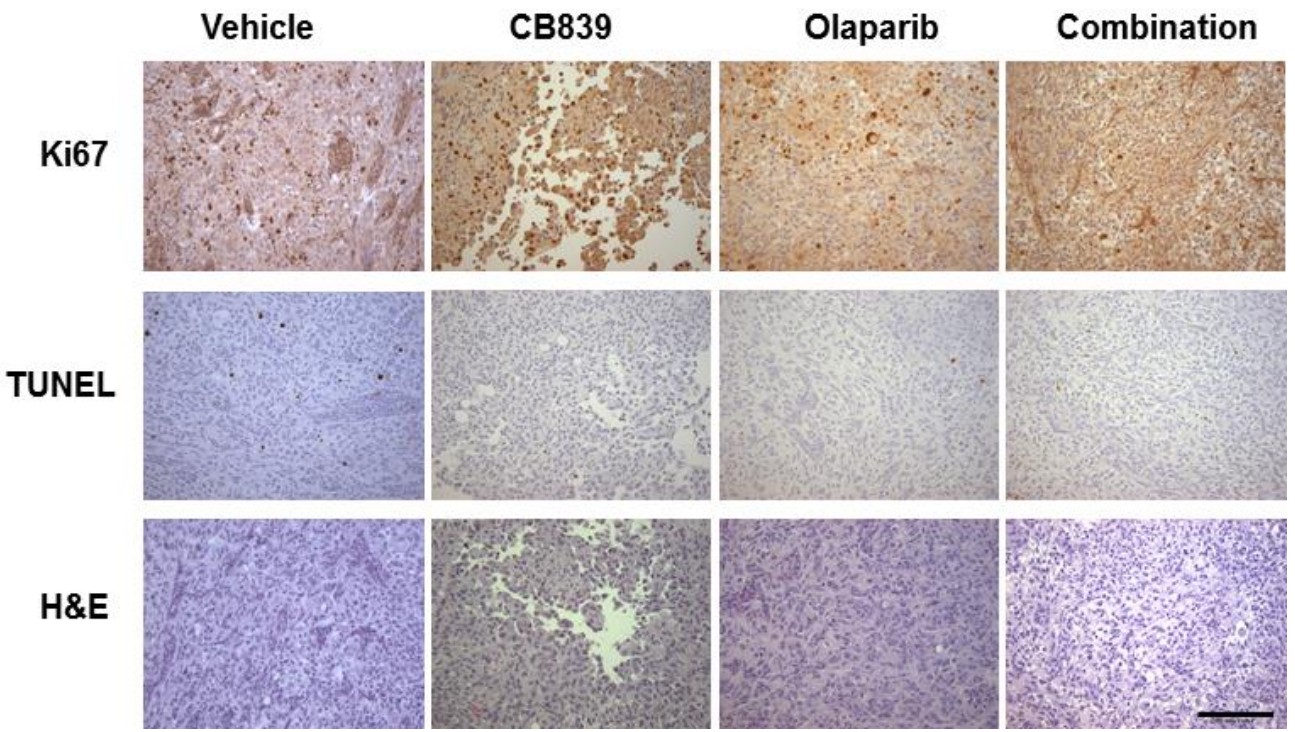

B

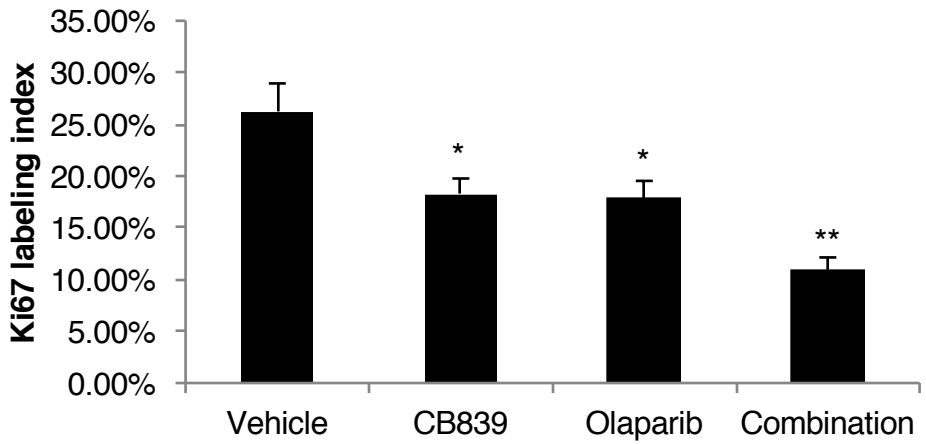

Supplementary Figure 16